

---

Erik Jonsson School of Engineering and Computer Science

---

2013-10-16

*In Situ Study of the Role of Substrate Temperature  
during Atomic Layer Deposition of HfO<sub>2</sub> on InP*

UTD AUTHOR(s): Hong Dong, KC Santosh, Xiaoye Qin, Barry Brennan,  
Stephen McDonnell, Dmitry Zhernokletov, Christopher L. Hinkle,  
Jiyoung Kim, Kyeongjie Cho and Robert M. Wallace

©2013 AIP Publishing LLC

## In situ study of the role of substrate temperature during atomic layer deposition of HfO<sub>2</sub> on InP

H. Dong, Santosh, K.C., X. Qin, B. Brennan, S. McDonnell, D. Zhernokletov, C. L. Hinkle, J. Kim, K. Cho, and R. M. Wallace

Citation: *Journal of Applied Physics* **114**, 154105 (2013); doi: 10.1063/1.4825218

View online: <http://dx.doi.org/10.1063/1.4825218>

View Table of Contents: <http://scitation.aip.org/content/aip/journal/jap/114/15?ver=pdfcov>

Published by the AIP Publishing

---

### Articles you may be interested in

In situ atomic layer deposition study of HfO<sub>2</sub> growth on NH<sub>4</sub>OH and atomic hydrogen treated Al<sub>0.25</sub>Ga<sub>0.75</sub>N  
*J. Appl. Phys.* **113**, 244102 (2013); 10.1063/1.4812243

In situ study of HfO<sub>2</sub> atomic layer deposition on InP(100)  
*Appl. Phys. Lett.* **102**, 171602 (2013); 10.1063/1.4803486

In situ synchrotron based x-ray fluorescence and scattering measurements during atomic layer deposition: Initial growth of HfO<sub>2</sub> on Si and Ge substrates  
*Appl. Phys. Lett.* **98**, 231905 (2011); 10.1063/1.3598433

An in situ examination of atomic layer deposited alumina/InAs(100) interfaces  
*Appl. Phys. Lett.* **96**, 202905 (2010); 10.1063/1.3432749

The initial atomic layer deposition of Hf O<sub>2</sub> Si ( 001 ) as followed in situ by synchrotron radiation photoelectron spectroscopy  
*J. Appl. Phys.* **104**, 064116 (2008); 10.1063/1.2978362

---



**AIP** | Journal of  
Applied Physics

*Journal of Applied Physics* is pleased to  
announce **André Anders** as its new Editor-in-Chief

# ***In situ* study of the role of substrate temperature during atomic layer deposition of HfO<sub>2</sub> on InP**

H. Dong,<sup>1</sup> Santosh, K.C.,<sup>1</sup> X. Qin,<sup>1</sup> B. Brennan,<sup>1</sup> S. McDonnell,<sup>1</sup> D. Zhernokletov,<sup>2</sup> C. L. Hinkle,<sup>1,2</sup> J. Kim,<sup>1</sup> K. Cho,<sup>1,2</sup> and R. M. Wallace<sup>1,2,a)</sup>

<sup>1</sup>Department of Materials Science and Engineering, University of Texas at Dallas, Richardson, Texas 75080, USA

<sup>2</sup>Department of Physics, University of Texas at Dallas, Richardson, Texas 75080, USA

(Received 6 September 2013; accepted 30 September 2013; published online 16 October 2013)

The dependence of the “self cleaning” effect of the substrate oxides on substrate temperature during atomic layer deposition (ALD) of HfO<sub>2</sub> on various chemically treated and native oxide InP (100) substrates is investigated using *in situ* X-ray photoelectron spectroscopy. The removal of In-oxide is found to be more efficient at higher ALD temperatures. The P oxidation states on native oxide and acid etched samples are seen to change, with the total P-oxide concentration remaining constant, after 10 cycles of ALD HfO<sub>2</sub> at different temperatures. An (NH<sub>4</sub>)<sub>2</sub>S treatment is seen to effectively remove native oxides and passivate the InP surfaces independent of substrate temperature studied (200 °C, 250 °C and 300 °C) before and after the ALD process. Density functional theory modeling provides insight into the mechanism of the changes in the P-oxide chemical states. © 2013 AIP Publishing LLC. [<http://dx.doi.org/10.1063/1.4825218>]

## **INTRODUCTION**

Metal oxide semiconductor field effect transistors (MOSFETs) based on III-V channel materials are strong contenders to replace the Si channel beyond the 20 nm node.<sup>1</sup> Buried channel In<sub>0.53</sub>Ga<sub>0.47</sub>As MOSETs using InP as a barrier layer between the high mobility channel and a high-k dielectric have shown improved electrical performance over surface channel devices by effectively moving the channel away from the oxide interface, which can minimize interfacial defects due to the oxidation of the channel.<sup>2,3</sup> However, the quality of the interface between the high-k dielectric and the InP barrier layer can still strongly impact the electrical performance of these devices, for example, by increasing the subthreshold swing.<sup>4</sup> It is well known that the density of interface states ( $D_{it}$ ) of III-V semiconductors are strongly correlated to the native oxides,<sup>5</sup> and In-P-oxides have been correlated to  $D_{it}$  for high-k/InP system.<sup>6</sup> Therefore, it is desirable to decrease the native oxide concentration on the InP surface in order to improve electrical performance.<sup>7</sup>

One of the advantages of high-k dielectrics grown by atomic layer deposition (ALD) on III-V substrates is the “self cleaning” effect,<sup>7</sup> in which the native oxides are converted by the first pulse of metal precursor during ALD.<sup>8,9</sup> Suri *et al.* have shown, using tetrakis(dimethylamido)hafnium (TDMA-Hf) and H<sub>2</sub>O precursors, that the “self cleaning” effect on GaAs is temperature dependent, with the removal of oxides being more pronounced at 300 °C than at the 250 °C or 200 °C.<sup>10</sup> However, quite different trends for the “self cleaning” effect have been reported on GaAs in comparison to those for acid etched and S-passivated InP.<sup>9,11,12</sup> A less efficient “self cleaning” effect has been observed during thin film deposition (2 nm) of ALD HfO<sub>2</sub>, while the “self cleaning” effect has been reported to be

enhanced significantly following thick (8 nm) ALD using tetrakis(ethylmethylamino)hafnium (TEMA-Hf) and water as precursors at a substrate temperature of 300 °C.<sup>7</sup> Recently, An *et al.*<sup>13</sup> reported the impact of ALD temperature on HfO<sub>2</sub> deposition on S-passivated InP substrates using TEMA-Hf and water, with a significant “self cleaning” effect occurring at 200 °C and 250 °C but substantial InP substrate oxidation occurring at 300 °C.<sup>13</sup>

This apparent variation during ALD HfO<sub>2</sub> on different III-V substrate materials therefore warrants further study. In addition, most previous studies on InP have been carried out using *ex situ* ALD, and spurious reactions may occur due to atmospheric exposure. In particular, interfacial oxide regrowth during air exposure could potentially lead to errors in interpreting reaction mechanisms.<sup>14</sup> Actually, recent *in situ* “half cycle” studies of ALD HfO<sub>2</sub> and Al<sub>2</sub>O<sub>3</sub> on native oxide and chemically treated InP (100) have shown that no “self cleaning” effect takes place on P-oxides during the initial ALD process.<sup>9,15</sup> In this study, the *in situ* evolution of a high-k/native oxide and wet chemically treated InP (100) interface during ALD at temperatures of 200 °C, 250 °C, and 300 °C is reported, and the role of ALD temperature in the removal of InP (100) interfacial oxides during the initial stages using TDMA-Hf and water is investigated.

## **EXPERIMENTAL**

Three sets of *n*-type S-doped InP (100) samples with a doping concentration of  $1 \times 10^{18}/\text{cm}^3$  were used in this work. All of the samples were degreased with acetone, methanol, and isopropanol for 1 min each at room temperature before further wet chemical treatment. Each of the three sets consisted of one sample degreased only (native oxide); one sample degreased and cleaned using a two step piranha (acid etch), H<sub>2</sub>SO<sub>4</sub>:H<sub>2</sub>O<sub>2</sub>:H<sub>2</sub>O = 4:1:100 for 2 min, then H<sub>2</sub>SO<sub>4</sub>:H<sub>2</sub>O = 1:1 for 30 sec, where the initial concentrations

<sup>a)</sup>Electronic mail: [rmwallace@utdallas.edu](mailto:rmwallace@utdallas.edu)

of  $\text{H}_2\text{SO}_4$  and  $\text{H}_2\text{O}_2$  were 96% and 30%, respectively,<sup>16</sup> and a final sample was degreased and treated with 10% aqueous  $(\text{NH}_4)_2\text{S}$  solution for 20 mins (S-pass).<sup>17</sup> Each sample set was mounted onto a separate titanium plate to allow ALD to be carried out on all three samples within a given set simultaneously. Wet chemical treatments were coordinated so that sample exposure time to atmosphere was minimized for all samples prior to loading in ultrahigh vacuum (UHV) (less than 6 min).

The experiment was performed in a UHV cluster tool, described in detail elsewhere,<sup>18</sup> consisting of a Picosun ALD reactor and an X-ray photoelectron spectroscopy (XPS) analysis chamber, connected by a UHV transfer tube maintained at a pressure of less than  $2 \times 10^{-10}$  mbar, which allowed samples to be transferred between the deposition and analysis chambers without exposure to atmosphere. Ten cycles of ALD  $\text{HfO}_2$  were grown in the ALD chamber using TDMA-Hf and water as precursors with a 0.1 s/20 s/0.1 s/20 s sequence of TDMA-Hf/purge/water/purge. High purity  $\text{N}_2$  gas was used as both the carrier and purge gas. The only variation in the ALD conditions was the substrate temperature which was set to 200 °C, 250 °C, or 300 °C for the three different sample plates. The pressure in the ALD chamber during the deposition was about 10 mbar.<sup>8</sup> XPS was carried out using a monochromatic Al  $K\alpha$  ( $h\nu = 1486.7$  eV) X-ray source. XPS scans were taken at 45° with respect to the sample surface normal, with an electron pass energy of 15 eV and a seven channel hemispherical analyzer. In  $3d_{5/2}$ , P  $2p$ , O  $1s$ , C  $1s$ , S  $2p$ , Hf  $4d$ , Hf  $4f$ , and In  $4d$  core level spectra were analyzed to study the interfacial oxide after 10 cycles of ALD  $\text{HfO}_2$ . To compensate for charging effects or band bending induced binding energy shifts, all fitted spectra for each set of samples were referenced to the P  $2p$  bulk peak at 129 eV.<sup>19</sup>

First principles calculations based on density functional theory (DFT) with projector augmented wave pseudopotentials implemented in the Vienna *Ab-initio* Simulation Package<sup>20</sup> were used in order to better understand the atomic structures of the native oxides present on the InP surface. The electronic wave functions were represented by plane wave basis sets with a cutoff energy of 450 eV. The exchange correlation interactions were incorporated as a functional of generalized gradient approximation (GGA).<sup>21</sup> The atomic positions were allowed to relax while the cell sizes were kept fixed. A Monkhorst pack of  $4 \times 4 \times 4$   $k$ -point mesh was used in the structure relaxation and self-consistent calculations (SCF). The unit cells of  $\text{InPO}_4$  and  $\text{In}(\text{PO}_3)_3$  oxide states were relaxed and optimized with tolerances of  $10^{-4}$  eV and 0.01 eV/Å, the energy and force convergence, respectively.

## RESULTS AND DISCUSSION

Figure 1 shows In  $3d_{5/2}$  XPS spectra for (a) native oxide, (b) acid etched, and (c) S-passivated samples before ALD and after 10 cycles of  $\text{HfO}_2$  ALD at substrate temperatures of 200 °C, 250 °C and 300 °C. The “No ALD” spectra are representative of the spectra acquired from each sample on the three sample plates prior to  $\text{HfO}_2$  deposition. The peaks

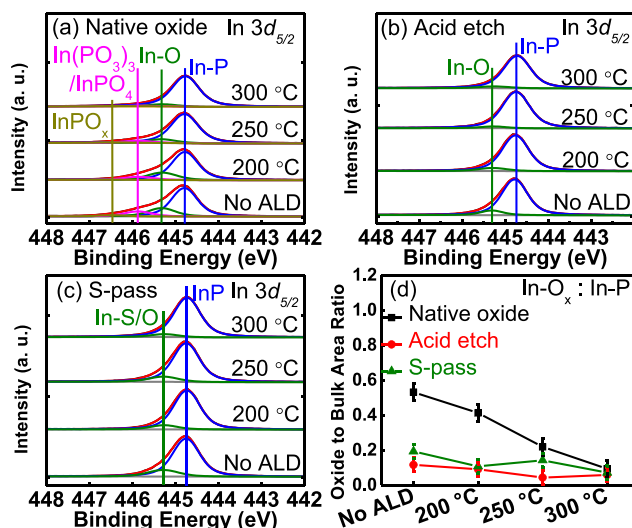


FIG. 1. In  $3d_{5/2}$  core level spectra before ALD and after 10 cycles of ALD  $\text{HfO}_2$  at 200 °C, 250 °C and 300 °C, for the (a) native oxide, (b) acid etched and (c) S-passivated by  $(\text{NH}_4)_2\text{S}$  treatment InP (100) samples. (d) Total In-oxide peak to InP bulk peak area ratios for all samples at all ALD temperatures.

with binding energy separations of +0.54 eV, +1.1 eV, and +1.7 eV relative to the In-P bulk peak are assigned to an In-O (In-S/O for the S-passivated sample) and are possibly related to  $\text{In}_2\text{O}_3$ ,<sup>22</sup> a component made up of  $\text{InPO}_4$  and  $\text{In}(\text{PO}_3)_3$  states (which is difficult to resolve due to the small variation in binding energy between these two states), and  $\text{InPO}_x$ .<sup>9,23</sup> Figure 1(d) shows In-oxides to InP bulk peak ratios from the native oxide, acid etch and S-passivated samples with no ALD, and ALD at 200 °C, 250 °C and 300 °C. For the native oxide and acid etched samples, the In-oxide concentrations are seen to decrease minimally after 10 cycles of  $\text{HfO}_2$  growth at 200 °C, significantly at 250 °C, and nearly completely at 300 °C. This suggests that TDMA-Hf is more reactive at a higher ALD temperature, such that the “self cleaning” is more effective at decreasing the In-oxide concentration. For the S-passivated sample, the In-S/O concentration is very small and does not change significantly after ALD at different temperatures.

Figure 2 shows the P  $2p$  spectra from the (a) native oxide, (b) acid etched, (c) S-passivated samples, before ALD, and after 10 cycles of  $\text{HfO}_2$  ALD at 200 °C, 250 °C and 300 °C. The peak with a binding energy separation of +4.0 eV to the InP bulk peak is assigned to P-OH bonding;<sup>24</sup> the peak with a binding energy separation of +4.5 eV to the InP bulk peak is assigned to  $\text{InPO}_4$ , and the peak with a binding energy separation of +5.1 eV is assigned to  $\text{In}(\text{PO}_3)_3$ .<sup>19,23</sup> Figure 2(d) shows the ratio of the total P-oxide peak area to that of the InP bulk peak of each respective surface. The P-oxide concentration is the same for each individual treatment, within the experimental error, after 10 cycles of ALD at all temperatures (the “no ALD” spectra for each individual sample is not shown here). This indicates that there is no “self cleaning” of P-oxides during  $\text{HfO}_2$  deposition regardless of the ALD temperature and surface treatment. For the native oxide sample, where most P-oxides are present, the chemical compositions of the P-oxides are seen



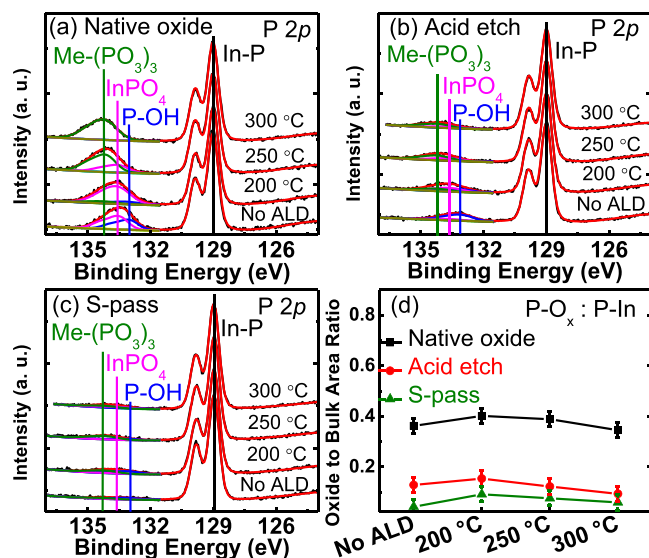


FIG. 2. P 2p core level spectra before ALD and after 10 cycles of  $\text{HfO}_2$  ALD at 200 °C, 250 °C and 300 °C, for the (a) native oxide, (b) acid etched and (c) S-passivated by  $(\text{NH}_4)_2\text{S}$  treatment InP (100) samples. (d) Total P-oxides peak to InP bulk peak area ratio for all samples at all ALD temperatures.

to change to higher binding energy and more phosphorous rich states with higher ALD temperatures. Specifically, the P-OH bonding concentration is seen to decrease significantly at all temperature, with  $\text{InPO}_4$  being the predominant state after 10 cycles of ALD at 200 °C. After 10 cycles of ALD at 250 °C, the  $\text{InPO}_4$  state is present at a lower concentration relative to that after ALD at 200 °C, and the  $\text{In(PO}_3)_3$  state emerges. After 10 cycles of ALD at 300 °C, the  $\text{In(PO}_3)_3$  state is the only oxide state detected. The concentrations of P-oxide on the acid etched and S-passivated samples are both low, and the minimum P-oxide concentration is found for the S-passivated samples, close to the limit of XPS detection, independent of the ALD temperature.

The larger decrease of In-oxide concentration and the lack of a decrease in P-oxide concentration at higher substrate temperatures during the initial stages of  $\text{HfO}_2$  ALD on InP are contradictory to previously reported *ex situ* analysis of thin  $\text{HfO}_2$  film (2 nm).<sup>11,13</sup> However, another *in situ* XPS report of ALD  $\text{HfO}_2$  “half cycle” at a substrate temperature of 250 °C has shown consistent results with this study, where the In-oxide concentration is seen to decrease and the P-oxide concentration remains constant during the initial ALD stages.<sup>15</sup> This contradiction between *ex situ* and *in situ* results from the thin oxide films (less than 2 nm) is possibly due to the interfacial oxide regrowth, and this oxidation is seen to be enhanced by increased substrate temperature upon removal from the ALD reactor.<sup>14</sup> With thicker oxide films (greater than 2 nm), this effect should be reduced, as the increased oxide thickness should be sufficient to prevent the diffusion of oxygen to the interface.

Figures 3(a) and 3(b) show the full width at half maximum (FWHM) of the In  $3d_{5/2}$  and P 2p of InP bulk peak from the native oxide, acid etched, and S-passivated samples before and after ALD at the different temperatures studied. The FWHM of both the In  $3d_{5/2}$  and P 2p from the native oxide and acid etched samples are not seen to change significantly

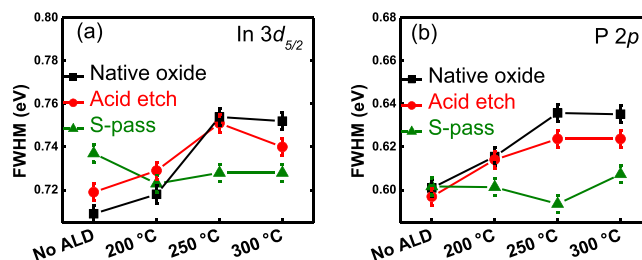


FIG. 3. InP bulk peak FWHM derived from In  $3d_{5/2}$  and P 2p spectra with no ALD, and with ALD at 200 °C, 250 °C, and 300 °C.

after ALD at 200 °C. However, an increase is evident after deposition at 250 °C and 300 °C, which is consistent with the ALD half cycle study of  $\text{HfO}_2$  on InP at 250 °C.<sup>15</sup> This increase in FWHM suggests that there is an increase in the number of bonding environments for these two samples, possibly due to increased surface disorder introduced during interaction with the TDMA-Hf precursor. However, the FWHM of the S-passivated InP samples are not seen to vary significantly with higher ALD temperature, suggesting that a more stable In-bonding environment is obtained by  $(\text{NH}_4)_2\text{S}$  treatment. Figure 3(b) shows the P 2p spectra FWHM of all samples before and after 10 cycles of ALD at the different temperatures. For the native oxide and acid etched samples, the FWHM is seen to increase minimally after ALD at 200 °C, and significantly increase after ALD at 250 °C, and 300 °C. The increases in FWHM again suggest that there is an increase in the number of bonding environments on the native oxide and acid etched samples after ALD due to interaction between the TDMA-Hf and In and P-oxides. The lack of increase in the FWHM of the bulk peaks suggests a more stable interface obtained from the S-passivated samples compared with those of the native oxide and acid etched samples.

Figure 4 shows the Hf 4d spectra on all samples after 10 cycles of ALD at different temperatures studied. The total amount of  $\text{HfO}_2$  growth is initially surface dependent. For the native oxide samples, much less  $\text{HfO}_2$  is grown at 200 °C than at 250 °C, and slightly less is grown at 250 °C than that

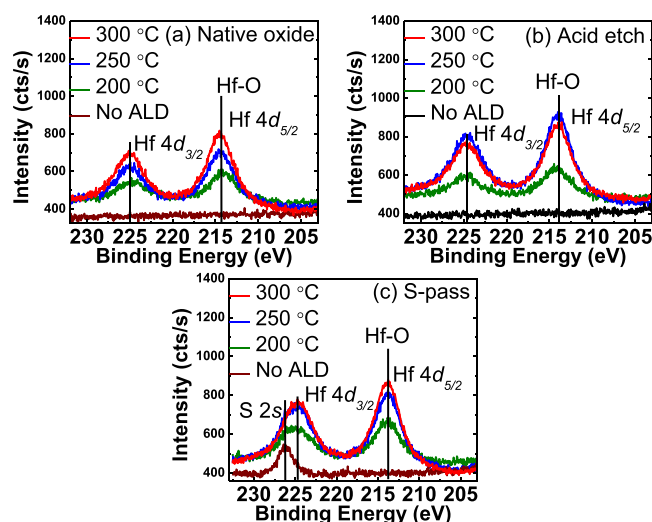


FIG. 4. Hf 4d core level spectra before ALD and after 10 cycles of ALD  $\text{HfO}_2$  at 200 °C, 250 °C, and 300 °C for (a) the native oxide, (b) acid etched, and (c) S-passivated InP samples.

at 300 °C. This is possibly because the TDMA-Hf precursor interacts with the In/P-oxide and forms HfO<sub>2</sub> more readily on the native oxide at increased ALD temperatures. For the S-passivated and acid etched samples, much less HfO<sub>2</sub> is deposited at 200 °C than at 250 °C and 300 °C, and the amount of HfO<sub>2</sub> deposited at 250 °C is similar to that at 300 °C. No S-Hf bond formation is observed upon ALD suggests that S does not play a role in affecting HfO<sub>2</sub> deposition on the S-passivated samples from the Hf 4*d* and S 2*p* spectra (not shown).

Figure 5 shows the O 1*s* spectra of the “no ALD” and after 10 cycles of ALD at different temperatures on the native oxide, acid etched, and S-passivated InP samples. The O chemical states of the native oxide sample are converted from a non-bridging O (P-O··In) rich state to a bridging O rich (P-O-P) state with higher ALD temperatures.<sup>19</sup> Much less P-oxide is observed for the S-passivated sample compared to the native oxide sample prior to ALD, which is consistent with the P 2*p* spectra.

Figure 6 shows the crystal structure of InPO<sub>4</sub> and In(PO<sub>3</sub>)<sub>3</sub> calculated by DFT and the simplified schematic of the PO<sub>4</sub> and PO<sub>3</sub> oxide units; the structures are the same as those reported by Sferco *et al.*<sup>25</sup> In each “PO<sub>4</sub>” unit, all four P and O bonds are non-bridging (P-O··In). There are two non-bridging bonds (P-O··In) and one bridging bond (P-O-P) on average per “PO<sub>3</sub>” unit, where each bridging O bond links two tetrahedral PO<sub>4</sub> units. Therefore, the O 1*s* spectra results suggest that InPO<sub>4</sub> is converted to In(PO<sub>3</sub>)<sub>3</sub> after ALD at higher temperature, which is likely facilitated by the loss of oxygen from a PO<sub>4</sub> unit to form a PO<sub>3</sub> unit and a Hf-O bond. Relative to In, In(PO<sub>3</sub>)<sub>3</sub> is more P-rich compared with InPO<sub>4</sub>, so more P-rich oxides formation is observed with higher ALD temperature in this study. This behavior is also consistent with that of the P 2*p* spectra. A possible reaction is as follows:

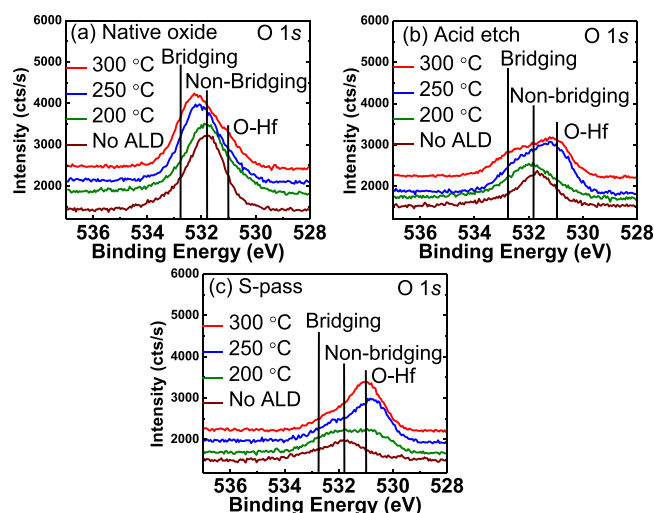
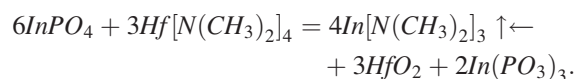


FIG. 5. O 1*s* core level spectra before ALD and after 10 cycles of ALD HfO<sub>2</sub> at 200 °C, 250 °C, and 300 °C from the (a) native oxide, (b) acid etched, and (c) S-passivated InP samples.

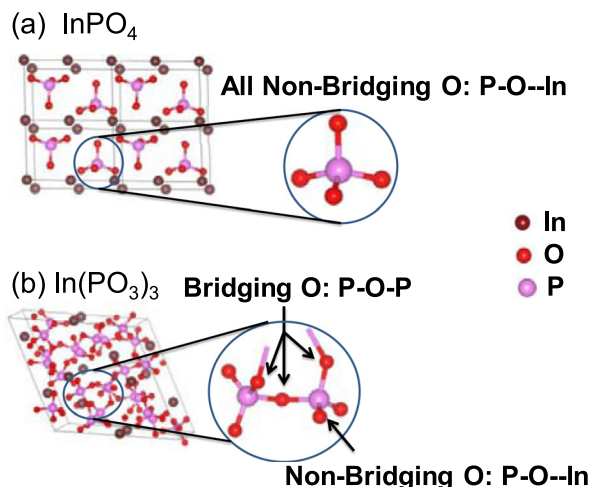


FIG. 6. Schematic of the structure of InPO<sub>4</sub> and In(PO<sub>3</sub>)<sub>3</sub>. All O in InPO<sub>4</sub> are non-bridging, and each In(PO<sub>3</sub>)<sub>3</sub> unit has two non-bridging O and two bridging O, which link two tetragonal PO<sub>4</sub> unit. Each PO<sub>3</sub> unit has an average of one bridging O.

ALD at a higher temperature may lower the energy barrier of this reaction, resulting in more significant decrease in concentration of In-oxides. Because the Hf is in direct contact with the P-oxides, formation of Hf-O-P bonding is also possible.

Previously, an electrical study presented evidence of the presence of P-rich oxides correlating with higher *D<sub>it</sub>* by a comparison of Al<sub>2</sub>O<sub>3</sub>/InP and HfO<sub>2</sub>/InP stacks based on post deposition anneal treatments.<sup>26</sup> Therefore, from the results in this study, a higher *D<sub>it</sub>* is expected due to more P-rich oxide formation at higher ALD temperatures. This is consistent with a recent report by An *et al.*,<sup>27</sup> that a significant degradation of electrical performance for HfO<sub>2</sub>/InP stack after ALD at 300 °C, compared with that for ALD at 200 and 250 °C. In addition, a recent DFT calculation has also suggested that the oxidation of In and P atoms at the (2 × 4) InP reconstructed surface induces the band gap states.<sup>28</sup> Considering the low growth rate of ALD at 200 °C, and the high *D<sub>it</sub>* expected from ALD at 300 °C, ALD of HfO<sub>2</sub> at 250 °C likely the optimum temperature to deposition HfO<sub>2</sub>. The persistence of P-oxides at the interface suggests that an optimized surface cleaning and passivation process prior to the ALD process is critical to obtain a high quality InP/HfO<sub>2</sub> interface suitable for device performance.

## CONCLUSIONS

In summary, the role of ALD HfO<sub>2</sub> temperature on the “self cleaning” effect of native oxide, acid etched and S-passivated InP (100) samples is studied by *in situ* XPS. For the native oxide and acid etched samples, a greater reduction in In-oxides by the “self cleaning” effect of the TDMA-Hf precursor is seen with the higher ALD temperature studied. However, the total concentration of P-oxide remains the same regardless of the ALD temperatures studied here. Instead, the chemical states of the P-oxides are seen to change with increasing ALD temperature. An increase in the number of bonding environments at the interface is detected after 10 cycles of HfO<sub>2</sub> growth at 250 °C and 300 °C on the native

oxide and acid etched samples, evidenced by an increase in the FWHM of both In  $3d_{5/2}$  and P  $2p$  core level spectra in the InP bulk peaks. Therefore, it is not possible to rely on the ALD “self cleaning” effect to remove the native oxide for device fabrication at any of the ALD temperatures studied. 250 °C is likely the optimum ALD of HfO<sub>2</sub> temperature for the temperatures studied in this work, in terms of the initial growth rate and the chemical states of the resulting P-oxides correlating with  $D_{it}$ . For the S-passivated sample, very low oxide concentration is observed before and after 10 cycles of ALD, independent of the deposition temperature, suggesting (NH<sub>4</sub>)<sub>2</sub>S treatment prior to ALD is beneficial to improve the high-k/InP interface.

## ACKNOWLEDGMENTS

The authors thank Professor Y. Chabal and Mr. W. Cabrera for useful discussions. This work was supported by National Science Foundation (NSF) under ECCS award # 0925844. J. Kim acknowledges financial support through a grant from the R&D Program for Industrial Core Technology funded by the Ministry of Trade, Industry, and Energy (MOTIE), Republic of Korea (Grant No. 10045216).

<sup>1</sup>J. A. del Alamo, *Nature* **479**, 317–323 (2011).

<sup>2</sup>M. Radosavljevic, G. Dewey, J. M. Fastenau, J. Kavalieros, R. Kotlyar, B. Chu-Kung, W. K. Liu, D. Lubyshev, M. Metz, K. Millard, N. Mukherjee, L. Pan, R. Pillarisetty, W. Rachmady, U. Shah, and R. Chau, *IEEE Int. Electron Devices Meet.* **2009**, 1.

<sup>3</sup>J. Lin, T.-W. Kim, D. A. Antoniadis, and J. A. del Alamo, *Appl. Phys. Express* **5**, 064002 (2012).

<sup>4</sup>J. J. Gu, A. T. Neal, and P. D. Ye, *Appl. Phys. Lett.* **99**, 152113 (2011).

<sup>5</sup>C. L. Hinkle, M. Milojevic, B. Brennan, A. M. Sonnet, F. S. Aguirre-Tostado, G. J. Hughes, E. M. Vogel, and R. M. Wallace, *Appl. Phys. Lett.* **94**, 162101 (2009).

<sup>6</sup>R. V. Galatage, H. Dong, D. M. Zhernokletov, B. Brennan, C. L. Hinkle, R. M. Wallace, and E. M. Vogel, *Appl. Phys. Lett.* **99**, 172901 (2011).

<sup>7</sup>C. L. Hinkle, A. M. Sonnet, E. M. Vogel, S. McDonnell, G. J. Hughes, M. Milojevic, B. Lee, F. S. Aguirre-Tostado, K. J. Cho, H. C. Kim, J. Kim, and R. M. Wallace, *Appl. Phys. Lett.* **92**, 071901 (2008).

<sup>8</sup>M. Milojevic, C. L. Hinkle, F. S. Aguirre-Tostado, H. C. Kim, E. M. Vogel, J. Kim, and R. M. Wallace, *Appl. Phys. Lett.* **93**, 252905 (2008).

<sup>9</sup>B. Brennan, H. Dong, D. Zhernokletov, J. Kim, and R. M. Wallace, *Appl. Phys. Express* **4**, 125701 (2011).

<sup>10</sup>R. Suri, D. J. Lichtenwalner, and V. Misra, *Appl. Phys. Lett.* **96**, 112905 (2010).

<sup>11</sup>Y. S. Kang, C. Y. Kim, M.-H. Cho, K. B. Chung, C.-H. An, H. Kim, H. J. Lee, C. S. Kim, and T. G. Lee, *Appl. Phys. Lett.* **97**, 172108 (2010).

<sup>12</sup>C.-H. An, Y.-C. Byun, M. S. Lee, and H. Kim, *J. Electrochem. Soc.* **158**, G242 (2011).

<sup>13</sup>C.-H. An, Y.-C. Byun, M. S. Lee, and H. Kim, *Phys. Status Solidi (RRL)* **6**, 211–213 (2012).

<sup>14</sup>S. McDonnell, H. Dong, J. Hawkins, B. Brennan, M. Milojevic, F. Aguirre-Tostado, D. Zhernokletov, C. Hinkle, J. Kim, and R. Wallace, *Appl. Phys. Lett.* **100**, 141606 (2012).

<sup>15</sup>H. Dong, B. Brennan, D. Zhernokletov, J. Kim, C. L. Hinkle, and R. M. Wallace, *Appl. Phys. Lett.* **102**, 171602 (2013).

<sup>16</sup>Y. Sun, Z. Liu, F. Machuca, P. Pianetta, and W. E. Spicer, *J. Appl. Phys.* **97**, 124902 (2005).

<sup>17</sup>B. Brennan, M. Milojevic, C. L. Hinkle, F. S. Aguirre-Tostado, G. Hughes, and R. M. Wallace, *Appl. Surf. Sci.* **257**, 4082 (2011).

<sup>18</sup>R. M. Wallace, *ECS Trans.* **16**, 255 (2008).

<sup>19</sup>G. Hollinger, E. Bergignat, and J. Joseph, *J. Vac. Sci. Technol. A* **3**, 2082 (1985).

<sup>20</sup>W. Kohn and L. J. Sham, *Phys. Rev.* **140**, A1133 (1965).

<sup>21</sup>J. Perdew, K. Burke, and M. Ernzerhof, *Phys. Rev. Lett.* **77**, 3865 (1996).

<sup>22</sup>B. Brennan and G. Hughes, *J. Appl. Phys.* **108**, 053516 (2010).

<sup>23</sup>M. Faur, M. Faur, D. T. Jayne, M. Goradia, and C. Goradia, *Surf. Interface Anal.* **15**, 641 (1990).

<sup>24</sup>Y. Sun, Z. Liu, F. Machuca, P. Pianetta, and W. E. Spicer, *J. Vac. Sci. Technol. A* **21**, 219 (2003).

<sup>25</sup>S. J. Sferco, G. Allan, I. Lefebvre, M. Lannoo, E. Bergignat, and G. Hollinger, *Phys. Rev. B* **42**, 11232 (1990).

<sup>26</sup>R. V. Galatage, H. Dong, D. M. Zhernokletov, B. Brennan, and C. L. Hinkle, *Appl. Phys. Lett.* **102**, 132903 (2013).

<sup>27</sup>C.-H. An, C. Mahata, Y.-C. Byun, M. S. Lee, Y. S. Kang, M.-H. Cho, and H. Kim, *Phys. Status Solidi A* **210**, 1381 (2013).

<sup>28</sup>K. C. Santosh, W. Wang, H. Dong, K. Xiong, R. C. Longo, R. M. Wallace, and K. Cho, *J. Appl. Phys.* **113**, 103705 (2013).